Characteristics of the Magnetic System of Magnetic Bearing Biased with Permanent Magnets Attached to a Rotor

Satoru Fukata and Kazuyuki Yutani

Department of Energy and Mechanical Engineering, Kyushu University 36,
Fukuoka, 812-81, Japan.

Abstract: The characteristics of radially interacting magnetic systems are examined with respect to magnetic radial bearings consisting of permanent magnets for biasing and electromagnets for control. The permanent magnets with axial magnetization are positioned on a rotor and share the magnet poles with the electromagnets. The electromagnet coils of a pair of opposing stators are connected in series and are driven by a single power amplifier. The magnet cores are made of solid iron. The static and dynamical characteristics of the magnetic flux are measured with fixed airgap. The results are compared with the numerical results.

1. Introduction

The idea for active magnetic bearings composed of permanent magnets to provide bias force and electromagnets to supply control force has been considered for the reduction of the high cost and of the running energy consumption in the all electromagnetic design. A simple structure, which is similar to the all electromagnetic case in appearance, is the use of common magnet poles to the permanent magnets and the electromagnets. A key of this case is the construction of the magnetic circuits of the combined magnet system. The most reasonable way may be to position the permanent magnets at the stators[1]. This construction is advantageous for high speed, and makes it possible to combine the radial bearing with the thrust bearing. Another way is to attach the permanent magnets to a rotor[2]. In this case, since the composition of the rotor becomes complicated, there may be some problems to the rigidity of the shaft and to the elaborate machining of the rotor.

In these cases, however, a pair of opposing stator-coils across the rotor is connected in series and is driven by a single power amplifier. Therefore, the two magnet systems in the radial direction are prone to interact each other, and their characteristics become much more complicated than in the all electromagnetic case. The analysis was tried with the application of the magnetic circuit theory in [2] and [3] in the case of the permanent magnets attached to a rotor. Linearized dynamical equations were presented in [2] with the same dimensions of a pair of opposing magnet stator-coils. The analysis becomes much more complicated with the different dimensions of the stator-coils as in [3].

In this paper, we examine first experimentally the statical and dynamical characteristics of the magnetic system locating the permanent magnet at the rotor with fixed airgap. Next, we compare the results with the numerical results to check the analysis in [3] and to understand the properties of the magnetic system theoretically.

2. Magnetic System

2.1 Experimental Setup

Figure 1 shows the mechanical part of the experimental set up that has a magnet system similar to magnetic radial bearings composed of permanent magnets(PMs) for biasing and electromagnets(EMs) for control. A PM (ferrite) ring with axial magnetization is attached to a non-ferromagnetic shaft and is held between two iron rings (the rotors of the magnet system). An EM consists of a pair of magnet coils that are wound around stators 1 and 2 positioned on the radially opposing sides: the pair of magnet coils is connected in series and driven by a single power amplifier. The EM system is constructed in each radial direction in the bearings; but here we do not consider the other one, for simplicity, *i.e.,* stators 3 and 4 have no exiting coil. We confirmed experimentally that there is no great difference.

The airgap lengths between the rotor and the stators are set with paper of required thickness and with the spindle of a micrometer head whose frame is fixed on the plate. All the components except for the magnet cores and for the micrometers are made of non-ferromagnetic materials.

All the magnet cores are made of solid iron, only for simplicity of manufacturing. The permanent magnet is composed of two pieces of thickness 6.5mm, outer diameter 38mm and inner diameter 21mm each. The magnetic data are unknown to the authors. The rotor cores have the outer diameter of 44mm, and the thickness of 12mm on the upper side and 14mm on the lower side. For the stators, the thickness is all the same of 10mm, but two different sizes of width are used: the smaller is 18mm (the face area is 1.85 cm^2), the larger is 27mm (one and half times the smaller, the face area 2.89 cm^2).

The magnet coil is 200 turns in each stator, and their resistance is about 0.63 Ω and 0.93 Ω for the smaller and larger stators, respectively. The EM is driven with a chopper-type power amplifier with the static input-output gain b =1.0A/V and the current feedback control gain $p \cong 140$V/A.

We consider several combinations of the stators as is shown later in **Table 1**. The airgap lengths are fixed all to about 0.65mm.

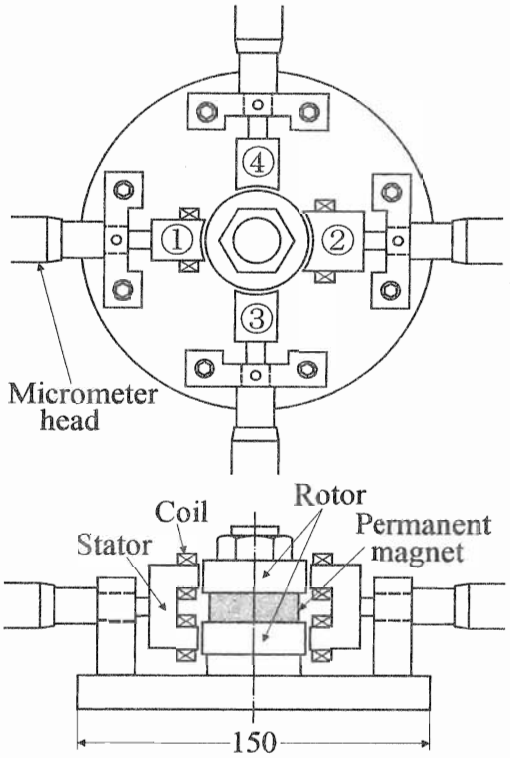

Fig.1 Experimental setup

2.2 Magnetic circuit

Figure 2 illustrates the main magnetic flux paths of the magnetic system. The permanent magnetic flux flows radially in the rotor and goes into the four poles of the stators through the airgaps, and passes through the stators along the axial direction to return to the rotor via the other airgaps. The electromagnetic flux generating from the two opposing magnet coils passes through the rotor along the radial direction with the total magnetic flux increasing on one side decreasing on the other side. The difference of the fluxes in the opposing sides produces control force.

Without flux saturation, the magnetic system may be modeled by the magnetic circuits as in **Fig. 3**, where

F_{mB} : imaginary magnetomotive force of PM

F_{mj} , f_{mj} : magnetomotive force

R_{mB} : magnetic internal resistance of PM.

R_{mj} : magnetic resistance

R_{mL} : magnetic resistance of leakage

Φ_j : magnetic flux.

The subscript j refers the flux path numbered corresponding to the stator. Magnetomotive forces due to eddy currents are considered here in the stators having non-exciting coil. The eddy currents are induced by the dynamical change of the magnetic fluxes that is caused by the alternating excitation of the magnet coils and/or the dynamical change of the airgaps. These effects may be neglected in the case of laminated magnet cores.

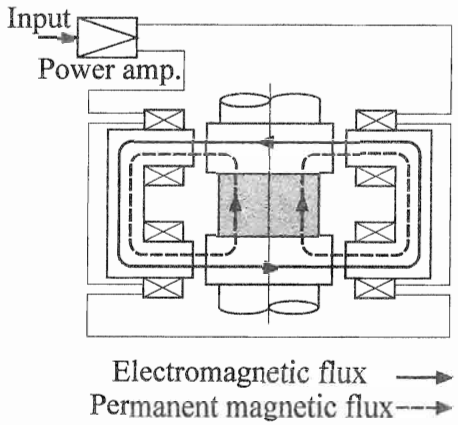

Fig. 2 Main paths of magnetic flux

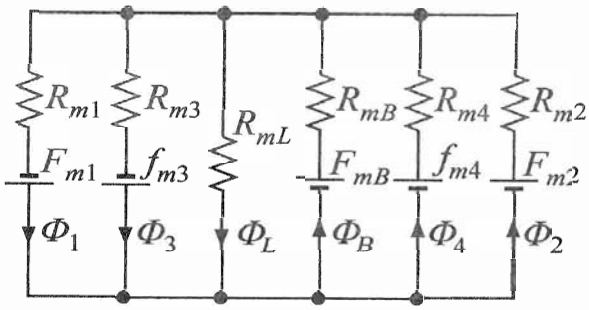

Fig. 3 Simplified magnetic circuits

3. Permanent Magnetic Flux

The static characteristics of permanent magnets may be considered along the demagnetization curve. This curve is quite linear for permanent magnets(PMs) made of ferrite or rare-earth material. Since we had no data of the PM, we estimate the residual magnetic flux density from the measurement, provided that the recoil permeability is equal to that of air.

3.1 Analytical Relations

We define the imaginary magnetomotive force and the magnetic internal resistance of a PM by[4]

$$F_{mB} = l_B \frac{B_r}{\mu_r}, \quad R_{mB} = \frac{l_B}{\mu_r A_B} \qquad (1)$$

where l_B is the thickness, B_r the residual magnetic flux density, μ_r the recoil permeability and A_B is the pole area. The magnetic resistance is estimated by

$$R_{mj} = \frac{2l_{mj0}}{\mu_0 A_j}, \quad A_j = (H + l_0)(W + l_0) \qquad (2)$$

where l_{mj0} is the equivalent airgap length considering

the magnetic path in the magnet core, μ_C the permeability of air, and A_j is the area with the airgap length of l_0 and the magnet pole of thickness H and circumferential width W.

From the analysis of the magnetic circuits in Fig. 3, we have the relation for the flux density [3]

$$B_j = \frac{\mu_0}{2l_{mj0}} \alpha_{TB} F_{mB} \tag{3}$$

where

$$\alpha_{TB} = \frac{R_T}{R_{mB}}, \qquad \frac{1}{R_T} = \frac{1}{R_S} + \frac{1}{R_{BL}},$$
$$\frac{1}{R_S} = \sum_{j=1}^{4} \frac{1}{R_{mj}}, \qquad \frac{1}{R_{BL}} = \frac{1}{R_{mB}} + \frac{1}{R_{mL}} \tag{4}$$

R_T is the parallel resistance of all the magnetic resistances. The relation to the residual flux density is obtained from eq. (1) as

$$\frac{B_j}{B_r} = \frac{\mu_0}{\mu_r} \frac{l_B}{2l_{mj0}} \alpha_{TB} \tag{5}$$

The relations (3) and (4) suggest that the flux density should depend on the airgap length if the magnetic resistance of the magnet core is negligible. From eq. (5) we have the relation for the two measurement cases with the equal airgap length as

$$c_B \equiv \frac{B_2}{B_1} = \frac{R_{T2}}{R_{T1}} = \frac{1 + R_{S1}/R_{BL1}}{R_{S1}/R_{S2} + R_{S1}/R_{BL2}} \tag{6}$$

It is difficult to obtain the leakage resistance R_{mL}. The value may vary with the experiment cases, to be exact, but if we assume it remains constant, then we have the following relation from eq. (6).

$$\frac{R_{BL}}{R_{S1}} = \frac{1 - c_B}{c_B(R_{S1}/R_{S2}) - 1} \tag{7}$$

3.2 Estimation of Unknown Data

The flux densities measured with a gaussmeter in the airgaps were nearly equal in each experiment case with the equal airgap length, as suggested in eq. (5). The average values are shown in Table 1 for three cases.

Assuming $\mu_r = \mu_0 = 4\pi \times 10^{-7}$ H/m, from eqs. (1) and (2) we have the magnetic resistances of $R_{mB} = 13.1 \times 10^6$ A/Wb and values shown in Table 2 later with the smaller and larger stators. Using these values with eqs. (4) and (7) for case 4 ($R_{m3} = R_{m4} = \infty$) and case 5 in Table 1, we obtain

$$R_{mL} = 3.9 \times 10^6 \text{ A/Wb} \cong 0.30\, R_{mB} \tag{8}$$

Then, from eqs. (3) and (5) we have

$$F_{mB} \cong 2600 \text{ A}, \qquad B_r \cong 0.25 \text{ T}$$

The values in parentheses in Table 1 are calculated from eq. (3) or (5) with this result.

As long as the flux saturation does not matter, the permanent magnetic flux may not affect on the generating electromagnetic flux. Considering that μ_r is nearly equal to μ_0, we may replace the PM with non-ferromagnetic materials to obtain the data with the electromagnet.

Table 1. Cases of experiment

Case	Stators ①	②	③	④	Flux density (T)	Response
1	L	L	×	×	0.220 (0.21)	Fig. 4
2	L	L	S	×		
3	S	S	×	×		Fig. 4
4	S	L	×	×	0.235 (0.24)	Fig. 5
5	S	L	S	S	0.160 (0.16)	Fig. 6

L : Larger S : Smaller × : Non

4. Electromagnetic Flux

To examine the dynamical characteristics of the magnetic flux, we measured the frequency responses by applying a non-biasing sinusoidal input with amplitude 0.6V to the power amplifier driving the electromagnet. This amplitude corresponds to the statical, incremental flux density of about 0.12T. We first obtained the frequency response of the generating voltage in a search coil, and then took the numerical integral operation to the result presented in complex number. The search coil of 4 (2 × 2) turns was wound around the two yokes of each stator near the airgap. The responses, especially for the phase, seem to be incorrect in low frequencies, as shown below. We guess that this is due to the FFT analysis without filtering the output signal.

4.1 Case of the same dimensions in the opposing stator-coils

First, we consider one electromagnet system consisting of the same dimensions and the same airgap length in the opposing stator-coils. With the larger stators, the frequency response of the magnetic flux is shown by solid lines in **Fig. 4** when stators 3 and 4 are removed (Case 1). The response was almost all the same as in the other stator. The arrangement of another stator (for example, Case 2) did not affect the response, as is suggested by the analysis of the magnetic circuits in Fig. 3.

With the smaller stators (Case 3), we had the response shown by solid lines in the figure. The result has the smaller gain with the smaller decay in higher frequencies, as is expected (the smaller stator gives the larger magnetic resistance and the smaller eddy current effects).

4.2 Case of different dimensions

Next, we examine the similar electromagnet system but with the stators of different size: the smaller one in stator 1 and the larger in stator 2 (Case 4). The responses of the incremental flux in the two stators were shown by solid lines in **Fig. 5**. We see that the incremental

fluxes are not equal, but that the frequency characteristics are nearly equal. The difference is statically about 1.7dB, absolutely 1.22.

With the former fact, it is supposed that a part of the flux generating in the larger stator does not enter the smaller stator and takes a shortcut through the permanent magnet, between the two rotors, etc. With the latter fact, compared with the results in Fig. 4, the gain becomes smaller in the larger stator, but larger in the smaller stator, decreasing their rate with frequency. Thus, the frequency characteristics become close to each other by compensating the characteristics of the other stator mutually. It is probably a chance that they are almost all the same.

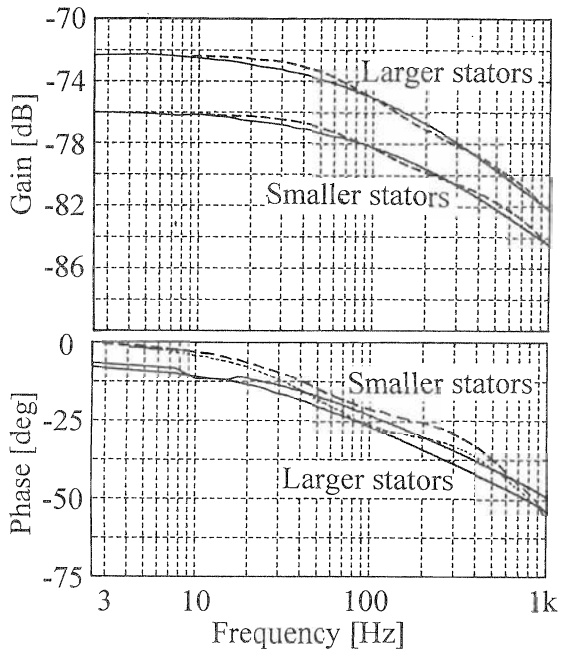

Fig. 4 Characteristics with the same dimensions (Cases 1 and 3)

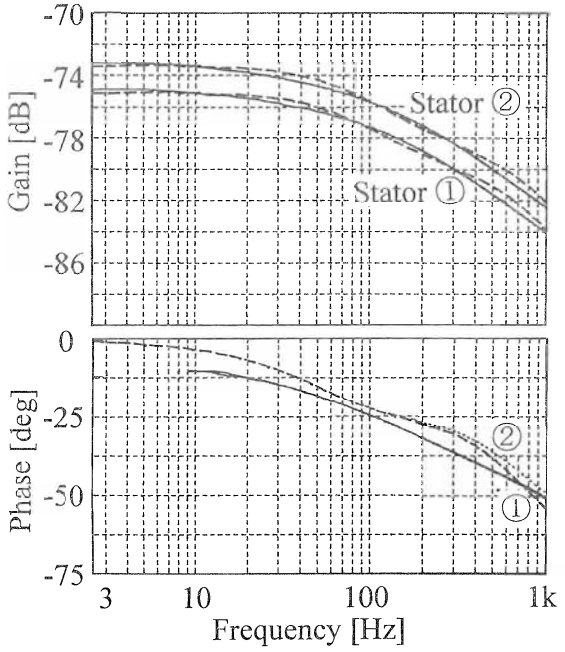

Fig. 5 Characteristics with different dimensions (Case 4)

4.3 Effects of Other Stators

Figure 6 gives the responses when stators 3 and 4 with the same dimensions are added at the place in Fig. 1 (Case 5). The features are summarized as follows:

(1) The incremental flux is larger in the larger stator than in the smaller stator, by 34% in the statical gain (the difference of 2.54dB, absolutely 1.34).

(2) A part of the magnetic flux flows into the stators of the other magnet system that is not excited. The absolute value is statically about 8% of that with the smaller exciting stator-coil.

(3) This rate decreases with frequency.

The rest of the flux of statically about 18% (=34-2 × 8) is considered to pass the shortcuts. The responses in higher frequencies are nearly equal to those of the case without the other stators (Case 4, Fig. 5), which is a result of item (3). Item (2) may be a natural result according to the principles of nature. Item (3) is supposed to be due to the eddy current effects in the stator.

5. Numerical Analysis

The magnetic circuit system in Fig. 3 was analyzed in [3] under similar conditions to those of the experiment case 5, with the first-order effects of eddy currents. Linearized equations describing the incremental flux were presented provided that both the variation of the

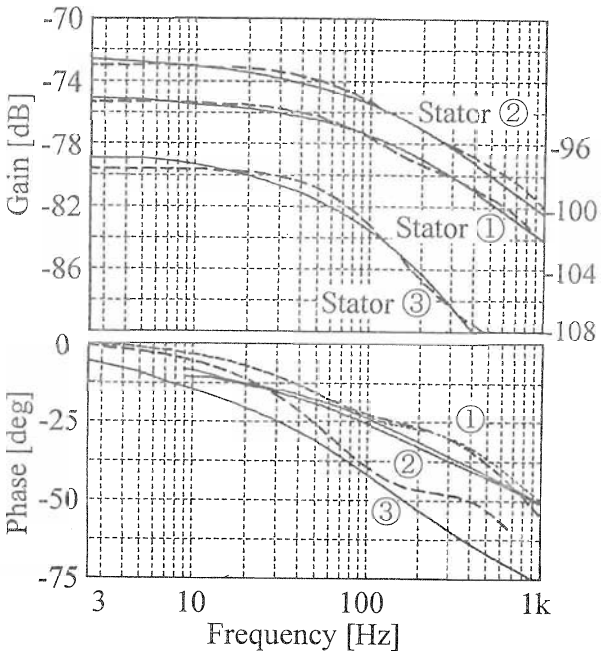

Fig. 6 Effects of other stators (Case 5)

airgap and the increment of the magnetic flux are sufficiently small. The results are valid for the larger increment of the magnetic flux when the airgap is fixed to be constant. We apply the results to obtain numerical results.

5.1 Analytical Results

Notations:

b : gain of power amplifier
e : input voltage to power amplifier
k : gain of magnetic flux
L : inductance of coil in one stator
N : turns of coil in one stator
p : feedback loop gain of current control
T_R : time constant with inductance of coil
T_L, T_{Le}, T_e : time constants with eddy currents
ϕ : incremental magnetic flux

$$k = b\frac{N}{R_m}, \quad L = \frac{N^2}{R_m}, \quad T_R = \frac{L}{p+R} \tag{9}$$

These are referred with subscript j corresponding to the stator.

With the equal dimensions of the opposing stator-coils without airgap variation, from a result in [2] or [3], we have the following relation with the Laplace transforms.

$$\frac{\Phi(s)}{E(s)} = k\frac{T_e s+1}{(T_1 s+1)(T_2 s+1)} \tag{10}$$

where the time constants T_1 and T_2 relate to the time constants with eddy currents as

$$T_L = T_1 T_2 / T_e - 2T_R,$$
$$T_{Le} = T_1 + T_2 - 2T_R - T_e \tag{11}$$

We note that the time constants T_R, T_e, T_L and T_{Le} are given for one-stator-coil system, and so the double term of T_R appears to be applied to the two-stator-coil system.

With the different dimensions of the opposing stator-coils, the relation becomes much more complicated[3]. For simplicity, we approximate this function with stator 1 by a simpler form similar to eq. (10) as

$$\frac{\Phi_1(s)}{E_1(s)} = k_1\beta_1\frac{\tilde{T}_{e1}s+1}{(\tilde{T}_{11}s+1)(\tilde{T}_{21}s+1)} \tag{12}$$

where $\tilde{T}_{e1}$, $\tilde{T}_{11}$ and $\tilde{T}_{21}$ are time constants to be identified, and β_1 is defined later in eq. (15).

For the incremental flux in stators 2 and 3 or 4 with the same input as to stator 1, from the results in [3] we obtain the following relations with the ratio to the incremental flux of stator 1.

$$\left.\frac{\Phi_2(s)}{\Phi_1(s)}\right|_{e_1} = c_{\alpha N}\frac{\beta_2}{\beta_1}\frac{T_{e2}s+1}{T_{e1}s+1} \cdot \frac{\frac{\alpha_{12}}{\beta_2}T_{L1}T_{e1}s^2 + \left(\frac{\alpha_{12}}{\beta_2}T_{Le1} + T_{e1}\right)s + 1}{\frac{\alpha_{12}}{\beta_1}T_{L2}T_{e2}s^2 + \left(\frac{\alpha_{12}}{\beta_1}T_{Le2} + T_{e2}\right)s + 1} \tag{13}$$

$$\left.\frac{\Phi_3(s)}{\Phi_1(s)}\right|_{e_1} = \frac{\alpha_3}{\beta_1}\frac{T_{e3}s+1}{(\tau_{e23}s^2 + \tau_{e13}s + 1)(T_{e1}s+1)} \cdot \frac{\tau_3 s^3 + \tau_2 s^2 + \tau_1 s + \bar{c}_{\alpha N}}{\frac{\alpha_{12}}{\beta_1}T_{L2}T_{e2}s^2 + \left(\frac{\alpha_{12}}{\beta_1}T_{Le2} + T_{e2}\right)s + 1} \tag{14}$$

where

$$c_{\alpha N} = \frac{\alpha_2}{\alpha_1}\frac{N_2}{N_1} = \frac{R_{m1}}{R_{m2}}\frac{N_2}{N_1}, \quad \bar{c}_{\alpha N} = 1 - c_{\alpha N},$$
$$\alpha_1' = (N_1/N_2)\alpha_1, \quad \alpha_2' = (N_2/N_2)\alpha_2,$$
$$\alpha_{12} = 1 - \alpha_1 - \alpha_2,$$
$$\beta_1 = 1 - \alpha_1 + \alpha_2', \quad \beta_2 = 1 + \alpha_1' - \alpha_2 \tag{15}$$
$$\tau_{e13} = (1 - 2\alpha_3)T_{Le3} + T_{e3},$$
$$\tau_{e23} = (1 - 2\alpha_3)T_{L3}T_{e3} \tag{16}$$
$$\tau_1 = T_{Le2} - c_{\alpha N}T_{Le1} + \bar{c}_{\alpha N}(T_{e1} + T_{e2}),$$
$$\tau_2 = (T_{L2}T_{e2} - c_{\alpha N}T_{L1}T_{e1}) + (T_{Le2}T_{e1} - c_{\alpha N}T_{Le1}T_{e2}) + \bar{c}_{\alpha N}T_{e1}T_{e2},$$
$$\tau_3 = (T_{L2} - c_{\alpha N}T_{L1})T_{e1}T_{e2} \tag{17}$$

For the same dimensions of the opposing stator-coils, we have $c_{\alpha N}=1$, $\bar{c}_{\alpha N}=0$, $\beta_1=\beta_2=1$, $\tau_1=\tau_2=\tau_3=0$ with the time constants of eddy currents being equal in the opposing sides. Then, the above equations give $\phi_2=\phi_1$ and $\phi_3=0$, which agrees with the experimental results.

Equation (13) explains how the dynamical characteristics of the magnetic flux become similar in the series connection of two stator-coils with the different dimensions. Equation (14) suggests that the leakage flux into the stators of the other magnet system decreases with frequency. As a special case, the dynamical characteristics are equal if the eddy-current effects are negligible.

5.2 Identification of Time Constants

Since it is difficult to estimate theoretically the time constants with eddy current effects, we obtain these experimentally by fitting eq. (10) into the frequency responses. In this case, T_R and k are calculated with eq. (9) and the turns of the search coil, 4, is considered in the statical gain. The identified values are shown in Table 2 for the cases of the larger stators (Case 1) and of the smaller stators (Case 3). Here, we selected the same values for T_1 and T_2, but different for T_e. The fitting curves are given in Fig. 4 by the broken lines.

5.3 Estimation of Leakage Resistance

The magnetic resistance of leakage R_{mL} was estimated in Section 3.2 with the measurement of flux density generated by the permanent magnet. We estimate it again from the statical gains of the frequency responses of case 4.

From eq. (12) with $R_{m3}=R_{m4}=\infty$ in eq. (4), we obtain the statical relation as

$$c_\phi \equiv \left.\frac{\phi_{20}}{\phi_{10}}\right|_{\substack{R_{m3}=\infty \\ R_{m4}=\infty}} = \frac{N_2}{N_1}\,\frac{1+\dfrac{N_1}{N_2}+\dfrac{R_{m1}}{R_{BL}}}{1+\dfrac{N_2}{N_1}+\dfrac{R_{m2}}{R_{BL}}} \qquad (18)$$

Then, we have

$$\frac{R_{m1}}{R_{BL}} = \frac{\left(1+\dfrac{N_1}{N_2}\right)\left(c_\phi - 1\right)}{1-\dfrac{c_\phi}{c_{\alpha N}}} \qquad (19)$$

Substituting c_ϕ=1.22, $N_1 = N_2$ and the values of R_{m1} and R_{mB} gives

$$R_{mL} = 3.2\times10^6 \text{ A/Wb} \cong R_{mB}/4 \qquad (20)$$

This is smaller by about 20% than that of eq. (8), and near to the resistance with the larger stator. Therefore, we should not disregard the leakage flux through it.

Table 2. Data of electromagnetic system

Stator	Smaller	Larger
subscript j	1	2
R_{mj} (A/Wb)	5.07×10^6	3.28×10^6
k_j (Wb/V)	3.95×10^{-5}	6.09×10^{-5}
T_{Rj} (ms)	0.056	0.086
T_{1j} (ms)	0.20	0.20
T_{2j} (ms)	2.0	2.0
T_{ej} (ms)	1.2	1.0
T_{Lj} (ms)	0.22	0.23
T_{Lej} (ms)	0.89	1.03

5.4 Numerical Results

For the experiment case 4, the frequency characteristic of the smaller stator (Fig. 5) is similar to that of case 3 (Fig. 4), and so it is fitted with the same values of $\tilde{T}_{11}$ and $\tilde{T}_{21}$ (see Table 2) and T_{e1}=1.15ms in eq. (12); the fitting response is shown by the broken lines in Fig. 5. Using this response and the relation with the time constants in Table 2 for the smaller and larger stators, we have the other broken lines in Fig. 5 with the larger stator.

For case 5, we take a similar procedure to the above. In this case, the experimental response of stator 1 is approximated with the same time constant as above (case 4), and drawn by the broken lines in Fig. 6. The broken lines of stator 2 are calculated based on eq. (13), and the broken lines of stator 3 are based on eq. (14) using the same time constants of eddy currents as stator 1 for stator 3.

We see that the relations of eqs. (13) and (14) fit well into the experimental results. This may show the validity of the analysis.

In practice, it is simple to have a similar expression to eq. (12) for all the stators. In this case, if we can select the same time constants of the denominator for the opposing sides, then we obtain a simpler dynamical expression for the resulting incremental force. The experimental results show this probability.

6. Conclusions

We considered the magnetic system consisting of permanent magnets to provide bias flux and of electromagnets to supply control flux. We attached the permanent magnets to a rotor and constructed the electromagnet with a pair of opposing stator-coils across the rotor. We measured the permanent magnetic flux and examined the dynamical characteristics of the incremental flux in each stator when we excite one electromagnet. The numerical results with identified data were compared with the experimental results to check the validity of the analysis and to give a reasonable understanding of the experimental results.

The primary characteristics of the magnetic system are summarized as follows:

(1) The two magnet systems in the radial direction interact each other in general. The magnetic flux may pass a shortcut and/or a bypass according to the principles of nature.

(2) The dynamical characteristics of the magnetic flux in the opposing sides become similar to each other, but not the same in general.

(3) In the case of solid magnet cores, the dynamical interaction decreases with increasing frequency.

(4) The magnetic resistance of the shortcut between the two rotor cores and in their vicinity is not negligible.

In the bearings, is more important the net force generated by the difference of the incremental fluxes in the opposing sides. Since the difference is less affected[3], the above characteristics have the less effect in practice. Anyway, the results suggest that the control force is prone to be influenced by the other control input. These characteristics are common to magnetic systems with a similar electromagnetic construction.

References

[1] Allaire, P.E.; *et al.*: Permanent Magnet Biased Magnetic Bearings-Design, Construction, and Testing, *Proc. 2nd Inter. Sympo. Magnetic Bearings*, pp. 175-182, Tokyo, June 1990.

[2] Fukata,S., and K.Yutani: Dynamics of Permanent-Magnet Biased Active Magnetic Bearings, *Proc. 3rd Inter. Sympo. Magnetic Suspension and Technology*, Tallahassee, Florida, 1995 (to be published).

[3] Fukata, S.: Analysis of Magnetic Circuits of Magnetic Bearings Biased with Permanent Magnet Attached to a Rotor, *Technology Report of Kyushu Univ.* (in Japanese), Vol. 69, No. 3, pp. 343-350, 1996.

[4] Ookawa, K.: *Introduction to Magnetic circuits of Permanent Magnets* (in Japanese), pp. 108-109, Sogo-Denshi Pub., Tokyo, 1994.